

mirrors, also developed by the XFD staff, as the first optical components in their beamlines. These too have performed as designed.

We are continuing to improve the performance of existing optical components, some of those programs are described in detail below, while simultaneously looking ahead to components capable of operation under even higher powers and power densities from enhanced storage ring performance, such as higher current and smaller vacuum chamber gaps, and/or 5-meter insertion devices. Although this study into higher power optical components is not yet complete, some of the initial results of that study have been included in this report.

## 5.3 X-ray Optics Development

### 5.3.1 Introduction

During the past years, the focus of the staff working on x-ray optics was almost exclusively on the development of high-heat-load monochromators and mirrors and their associated hardware. That work has paid off in the successful development of cryogenically cooled optical systems (crystals and liquid nitrogen pumps), water-cooled diamond monochromators, and contact-cooled mirrors with post-mirror, water-cooled monochromators. Many of the other CATs at the APS currently use cryogenically cooled silicon monochromators and a liquid nitrogen (LN<sub>2</sub>) pumping system, specified by XFD staff and first tested at the APS on the 1-ID beamline of SRI-CAT. To date, the cryogenic monochromators and pumps have performed very well with minimal lost beam time due to inadequate operation of the cryosystem. A few of the CATs have opted for a mirror-first geometry utilizing side-cooled silicon

Albeit the design and testing of high-heat-load optical components continue to occupy a good part of the time, some staff time has been allocated to x-ray optics developments not directly related to high-heat-load optical systems. Sagittally focusing crystals, x-ray interferometers, compound refractive lens, and use of gradient d-spacing crystals are but a few of the projects that are currently under development in XFD.

It should be pointed out that an important side benefit or spin-off of the high-heat-load monochromator development program was the establishment at the start of the program of a high-quality facility for the fabrication and characterization of single-crystal optical components. This facility continues to fabricate single-crystal optical components for high-heat-load optics development by XFD staff in addition to providing its services to all CATs at the APS. (See chapter 4 for more details on the capabilities and accomplishments of the x-ray optics fabrication and metrology laboratory.)

### 5.3.2 Cryogenically Cooled Silicon Monochromators

Cryogenically cooled silicon monochromators have been successfully in use at the 1-ID beamline for several years now. In the past year, our efforts have been directed towards improving the overall performance of the cooled monochromator system. Specifically, ongoing studies include investigation of the influence of geometrical parameters (i.e., crystal shape) on the performance of the component, cooling of the second crystal in the double-crystal monochromator (DCM) to reduce beam walk as a function of energy, and the use of liquid nitrogen reliquifiers to minimize the need to replenish the LN<sub>2</sub> supply. These studies are discussed in detail below.

Over the past year, we have initiated a program to explore the dependence of and to optimize the geometrical parameters on the thermal performance of the monochromator using finite element analyses (FEA). Our original design for a cryogenically cooled silicon monochromator called for a thin web to be fabricated on a robust block of silicon so that much of the incident beam power would be transmitted rather than being absorbed in the monochromator. An earlier experiment conducted by the high-heat-load team (Rogers et al., 1996), showed no difference in x-ray performance when the incident white beam impinged on the thin web or on a thick part of the silicon block (see Fig. 5.23). To better understand this, a model was developed to study the response of a simple block of cryogenically cooled silicon subjected to the same conditions as a thin one. The FEA results showed indeed that, under the current operational conditions, a simple cooled silicon block

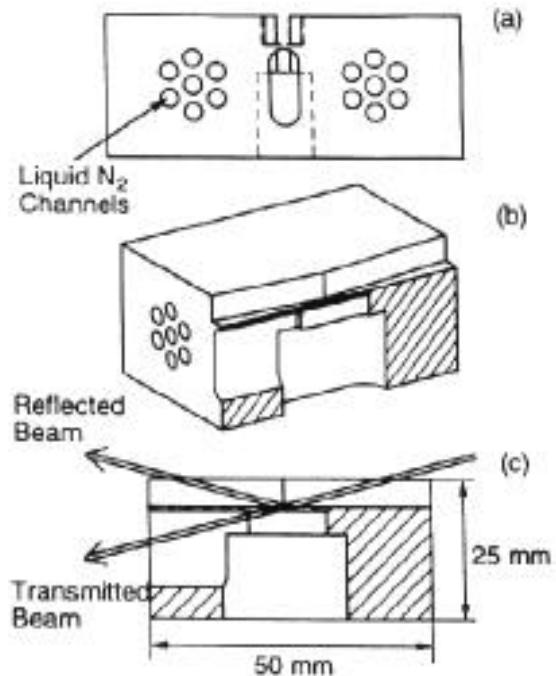


*Fig. 5.23 The original design for a cryogenically cooled silicon monochromator at the APS. A thin web was fabricated by milling a channel from the top of the block and removing material below the diffracting surface. This would allow a portion of the beam to pass through the monochromator and reduce the total heat absorbed. Experimental results showed that, at 100 mA and an undulator gap of 11 mm, the monochromator functioned perfectly even when the beam was allowed to strike the thick portion of the crystal (out of the channel on the top surface) resulting in a much higher absorbed power load.*

should perform as well, if not better, than one with a thin web fabricated into it. The magnitude of the mapping distortions depends on the cooling geometry and efficiency. In the case of a thin crystal, although less total heat is absorbed, heat flow is restricted by the dimension of the thin web, while in the thick crystal more

volume is available for the heat to spread, compensating for the additional absorbed power. In the case of a crystal made of a simple silicon block, the bowing component of distortion can be minimized by making the crystal as thick as possible; this may not be the case for the thin web design. Using a simple block leads to considerable saving in cost and fabrication time.

Other geometrical parameters being investigated include overall crystal size (2-D simulations showed the crystal size has to be as large as possible in order to spread the heat and lower the crystal temperature), the size of the thin portion of the crystal relative to the beam footprint (the thin web should be only slightly larger than the beam footprint), and the location of the beam on the thin web (the beam footprint should be as close possible to the crystal thick back wall).

To maintain the monochromatic beam parallel to the incident beam as a function of monochromatic beam energy (and hence have a true fixed offset monochromator), cryogenic cooling of the second crystal is necessary. Otherwise the d-spacing mismatch, due to the first crystal being at cryogenic temperature and the second crystal at room temperature, would cause the monochromatic beam to move (vertically) as a function of energy. For Si (111) crystals going from 6 keV to 18 keV, the motion is about 4 mm when the experiment station is 30 m from the monochromator. We have successfully implemented a cryogenic cooling scheme for the second crystal. This scheme involves directly cooling the second crystal mounting block (Invar) in a parallel plumbing arrangement with the first crystal. The second crystal is mounted on the cooling block via clamps and thermal contact is achieved via a layer of

indium/gallium. Although the indium/gallium layer freezes at cryogenic temperatures, it does not appear to strain the second crystal. Temperature measurements show that, during the initial crystal cool down of the DCM, both the first and second crystals show the same cooling behavior and both crystals reach cryogenic temperatures of  $\sim 90$  K in about 20 minutes. Furthermore, even though the second crystal stage is now connected to the first crystal via the additional cryogenic cooling lines, our measurements do not show any increase in flow-induced vibrations for the DCM system. However, due to the stiffness of the additional cryogenic cooling lines, the DCM is operated in a “fixed Z2” mode, in which the second crystal does not translate; the beam is allowed to walk on the face of the second crystal, which is 160 mm long. The measurements confirm that the monochromatic beam does indeed stay at a fixed height as the monochromator energy is varied over the range from 6 to 20 keV (see Fig. 5.24).

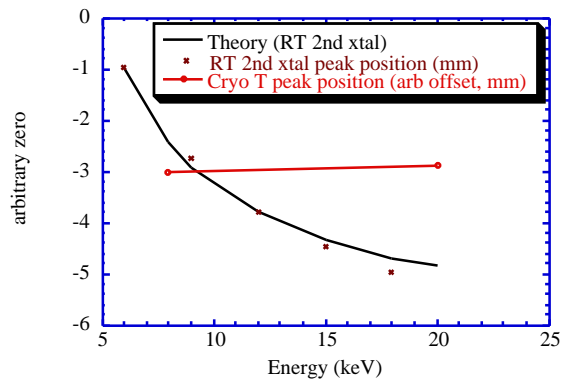


Fig. 5.24 Beam height in station 1-ID-C, as a function of the DCM energy, for a room temperature (RT, i.e., uncooled) second crystal (x) and a cryogenically cooled second crystal (o).

Although the application of cryogenic cooling has been an overwhelming success, the system does have some overhead associated with its operations. One of these overhead items is replacement of liquid nitrogen that has been lost from the system due to boil-off in the heat exchanger and to system losses. Depending on the cross-sectional size of the incident white beam and the setting of the undulator A gap, the cryogenic system requires approximately 180 liters of LN<sub>2</sub> per day. This 180 liters includes the system losses (through insufficient insulation, for example, and is estimated to be in the 80-100 W range) and, depending on the white-beam slit size and undulator gap, that due to the power absorbed by the crystal, which can be in excess of 500 W. (At the highest power, the system requirements can double to 360 liters per day.) Currently there is no distributed LN<sub>2</sub> in the experiment hall to provide for the LN<sub>2</sub> boil-off. Therefore to minimize the need to constantly change LN<sub>2</sub> supply dewars, we have been testing the use of reliquifiers to recapture the LN<sub>2</sub> boil-off. The reliquification system we have at present consists of two cold heads, each of which is capable of extracting 180 W from the gaseous nitrogen. As you can see, unless the undulator is running at a very large gap and/or with small slits, the capacity of the cold heads is not sufficient, and we still need to have a LN<sub>2</sub> supply tank to supplement the reliquifiers. However, with the addition of the reliquifiers, our need to change/resupply the LN<sub>2</sub> tanks has been considerably reduced from about one per day to about one every 3 or 4 days. Efforts to improve the reliability and efficiency of the cryogenic system continues with particular effort on improvements in the efficiency of the cryopumping system.

### 5.3.3 Diamond Monochromators

A water-cooled diamond high-heat-load monochromator was installed as a permanent component in the sector 3 ID beamline in May 1997. The monochromator consists of two synthetic type 1b diamond plates, 7 mm by 5.5 mm by 0.4 mm in size, oriented along the (111) direction. Recently a 5-mm (beam aperture) ID vacuum chamber, which allows a minimum undulator magnetic gap of 8.5 mm, was installed in the 3-ID beamline straight section. In this configuration, the calculated maximum power and surface power density from the 2.7-cm-period undulator that are absorbed by the first crystal are 20% and 35% larger, respectively, than for undulator A with a minimum gap of 11 mm. During the January 1998 run, we tested the thermal performance of the monochromator under this enhanced heat load. Figure 5.25 shows the measured FWHM of the (111) and (333) double-crystal rocking curves as a function of the energy of the (111) reflection, E(111). The undulator gap was changed so that the first harmonic energy corresponded with E(111). The calculated maximum absorbed power was 46 W at 10 keV (13.5-mm gap), and the calculated maximum absorbed surface power density was 6.8 W/mm<sup>2</sup> at 9 keV (12.4-mm gap). The absorbed power and surface power density decrease as a function of energy for E > 10 keV. We see no thermal effects on the measured FWHM as a function of the absorbed power or power density. One possible explanation for the increasing deviation from theoretical value of the (111) rocking curve FWHM as a function of energy is near-surface imperfections/defects in the crystals because the beam footprint on the crystal increases

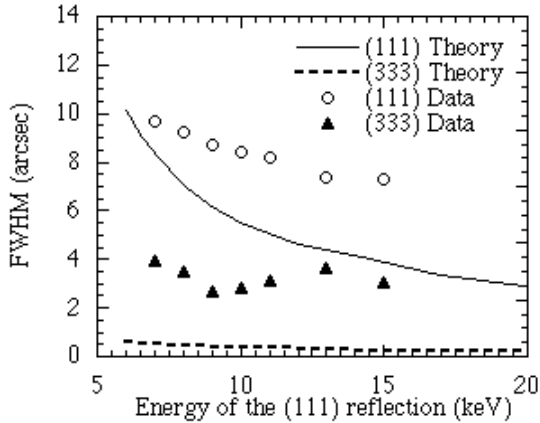


Fig. 5.25 Calculated and measured values for the FWHM of the diamond double-crystal rocking curves as a function of  $E(111)$ , the energy of the (111) reflection. Data were taken simultaneously for the (111) and (333) reflections; the energy of the (333) reflection is three times the abscissa value. The undulator gap ranged from 10.6 mm to 20.2 mm and was changed so that the first harmonic energy corresponded to  $E(111)$ . The storage ring current ranged from 93 to 90 mA.

as the energy increases. Such imperfections would be more noticeable in the (111) reflection than in the (333) reflection, since the former has a shorter extinction length.

Future plans for the diamond program include the evaluation of larger synthetic plates (8 mm by 5 mm) of type IIa that will be delivered by Sumitomo in late 1998, and the development of a cryogenic diamond monochromator for operation under the higher heat loads resulting from enhanced storage ring performance.

### 5.3.4 High-Heat-Load Optics for the Future (or Enhanced Storage Ring Operation)

Efforts have been continuing for many years now in developing analytical and numerical models to predict and optimize performance of high-heat-load monochromators for the APS. The method often used to calculate thermal and mechanical strains is finite element analysis (FEA). This technique in conjunction with simple mathematical models can provide very accurate predictions of the temperature, stress, and strain fields for complicated geometry and boundary conditions, which can then be used in diffraction simulation to calculate the rocking curve of the monochromator. This can save a considerable amount of time and money before building and testing of prototype monochromators. FEA modeling is particularly valuable when no adequate source is available for testing. Currently we are carrying out detailed thermal and structural finite element analyses to predict the performances of water-cooled diamond and liquid-nitrogen-cooled silicon monochromators under power loads that might be available under future operating conditions of the APS. Since it is difficult to predict with accuracy the future operational modes of the APS, we have chosen three scenarios that could be expected in the not-too-distant future (although scenario (a) in fact already exists on the 3-ID line). These are:

- a) an undulator with a 2.7-cm period and a minimum gap of 8.5 mm and 100-mA beam
- b) undulator A operating with a minimum gap of 8 mm and 100-mA stored beam

- c) undulator A operating with gap of 10.5 mm and 200-mA stored beam (This is equivalent to a 5-meter undulator with 100-mA stored beam.)

To date we have modeled only the current configurations of high-heat-load optical elements (cryogenically cooled silicon monochromators, water-cooled diamond monochromators, and side-cooled silicon mirrors). The monochromator energy range and ID gap combination are chosen so that they correspond to the worst case scenarios in term of absorbed surface power and power densities, and the beamlines are assumed to be windowless. We started out the modeling program looking at diamonds. We carried out simulations for two types of diamonds: type 1b and type IIa, using thermal conductivity values of 15 and 20 W/cm-K, respectively. The beam size is assumed to be 1.2 mm (vertical) by 2 mm (horizontal). The source parameters and power loads used in the FEA are given in Table 5.4.

The calculated (angular) distortions in all cases are smaller than the FWHM of the rocking curve of a perfect DCM. It is therefore expected that the water-cooled diamond monochromator performance will not be altered under the severe heat loads expected from future operating scenarios.

Work is ongoing for the cryogenically cooled silicon monochromators (a more difficult task due to the more complicated geometry and nonlinearities associated with the strongly temperature-dependent thermal conductivities and coefficients of thermal expansions). However initial results indicate that the current design may not be adequate for the highest powers and power densities being considered above.

While moderate heat load increases (up to about 30%) on the mirrors of present design can be tolerated at a cost of about a 50% increase in slope error, more significant increases in the heat load can lead to unacceptable temperature, slope errors, and stresses. We have embarked on improving

**Table 5.4 Parameters used for the FEA of the diamond monochromator. The absorbed power and power density are calculated for 0.4-mm-thick diamond and for 1.2 mm × 2 mm beam size at 30 m from the source.**

Source	Gap (mm)	K	E (keV)	Bragg Angle (deg.)	Current (mA)	Absorbed Power (W)	Surface heat flux (W/mm <sup>2</sup> )
Undulator A, period=2.7 cm	8.5	2.181	5.1	36.3	100	57	14.4
			17.0	10.2		94	7.1
Undulator A, period=3.3 cm	8.0	3.57	3.5	59.3	100	33	11.7
			17.0	10.2		72	5.4
Undulator A, period=3.3 cm	10.5	2.7	3.5	59.3	200	73	27.1
			17.0	10.2		149	11.2

the design of a contact-cooled mirror aimed at handling, with acceptable performance, up to three times the current heat load. The key features of this mirror design are (1) introduction of a pair of notches in the mirror substrate (see Fig. 4.8 in chapter 4) for a more effective establishment of thermal moment balance in the substrate, (2) replacement of the indium foil used as interstitial material (between the copper cooling and silicon mirror) with In/Ga eutectic for a more efficient heat transfer, and (3) increasing the cooling block width for reducing substrate temperature. Preliminary analyses indicate that incorporation of these three features would lead to a mirror with under 5- $\mu$ rad slope error and with a maximum temperature of about 80 °C for a three-fold increase in incident power and power density. Stress levels in such a mirror will be high, and a prototype should be made and tested under simulated heat-load conditions.

### 5.3.5 Other X-ray Optics Related Activities

#### Sagittal Focusing

Sagittal focusing enhances the capabilities of a beamline through an increase in the flux density (photons/sec/mm<sup>2</sup>) delivered at the sample position. We have built and tested a sagittal bender for the second crystal of the cryogenic monochromator in the 1-ID beamline. The bender produces a 1:1 horizontal focus of the source at the 1-ID-C station 60 m from the x-ray source. The bender mechanism is the same as the one that has been successfully implemented by SRI-CAT in the sector 1 BM beamline and by UNI-CAT in the sector 33 ID beamline, with some modifications required to make it

fit into the Kohzu monochromator tank in station 1-ID-A.

The bender accommodates a 114-mm-long by 40-mm-wide silicon (111) crystal. The 114-mm-long by 7-mm-wide region in the center of the crystal is 0.7 mm thick. On each side of the thin central web, the crystal is at least 10 mm thick. These thicker edges and the very long aspect ratio of the crystal act to suppress antiscaling bending of the diffracting portion of the crystal. The thin web is bent by the action of two PZTs, one at each end of the length of the crystal. A third PZT is located parallel to the long axis of the crystal and allows for cancellation of any twist introduced by the two curvature PZTs. The PZTs push against fixed micrometers, which are preloaded before installing the bender in the monochromator tank. The curvature PZTs have a maximum extension of 80 microns, which is adequate to focus the beam for energies up to 24 keV.

Tests were carried out on the mirror bender during the May 1998 run. To characterize the focus size, a 0.4-mm-wide horizontal slit was scanned through the beam. The slit was located in the 1-ID-C station, at 58.5 m from the center of the 1-ID straight section. The expected magnification for this geometry was 0.88. We tested the bender at 4 energies: 9, 12, 15, and 18 keV. Figure 5.26 shows the horizontal FWHM of the beam as function of the extension of the curvature PZTs for the 15-keV case. The minimum focus was achieved at a PZT extension of 65 microns, giving a FWHM of 0.74 mm. After deconvolving the slit size, the measured FWHM is 0.62 mm, which is in good agreement with the expected value of 0.68 mm. Figure 5.26 also shows the total intensity delivered by the sagittal crystal,  $I_0$ , and the peak intensity through the 0.4-mm-wide slits,  $I_1$ . The peak flux through the slits

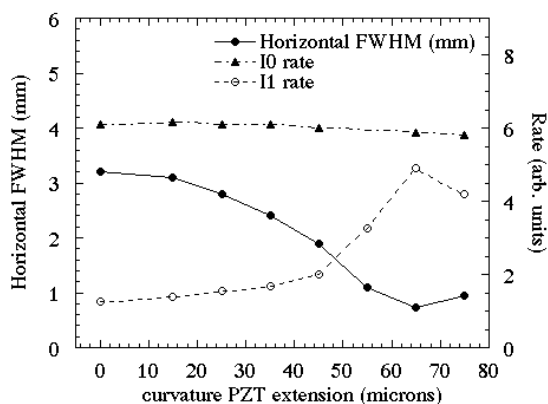


Fig. 5.26 Horizontal FWHM of the focused beam, total intensity  $I_0$  delivered by the bent crystal, and intensity  $I_1$  through the 0.4-mm-wide scanning slit as a function of the extension of the curvature PZTs.

$I_1$  increased by a factor of 4 from unfocused beam (0 micron extension) to focused beam (65 micron extension). The expected intensity gain in  $I_1$  was approximately 4.8, which is in reasonable agreement with the measurement. The total intensity  $I_0$  dropped by only 5%, indicating that the performance of the bent crystal is not degraded as the curvature is increased. Rocking curve measurements of the silicon (333) reflection also indicated that bending of the crystal does not affect the diffraction performance.

We obtained similar results and agreement with theory at the four energies studied. The average horizontal FWHM at the focus was 0.65 mm, while the average peak intensity gain through the 0.4-mm-wide slits was 3.9. The average loss in the flux delivered by the bent sagittal crystal was 7%. These tests showed that the sagittally focusing crystal performs well over an extended energy range. A problem that remains to be addressed is the thermal stability of the crystal/bender assembly. When the undulator beam impinges on the

cryogenically cooled first crystal, some of the incident power is scattered into the monochromator vacuum tank. A fraction of this scattered power is absorbed by the second-crystal assembly and results in thermal instability that alters the characteristics of the sagittal focus as a function of time. We plan to tackle this problem with a combined approach of shielding the second-crystal assembly to reduce the amount of absorbed power and of cooling or connecting the crystal/bender assembly to a heat sink.

## Compound Refractive Lenses

The compound refractive lens is a relatively new addition to the growing list of x-ray focusing optical components (Snigeriv et al., 1996). We have explored some of the potential uses for such a lens (Smither et al., 1997) and recently a prototype Be refractive lens was constructed for test purposes. The lens consisted of 50 hollow spheres machined into a Be substrate (Fig. 5.27). The web between each hollow sphere was 0.10 mm thick. The lens was made by machining hollow half spheres into two identical Be blocks and placing them together to make the row of hollow spheres. The lens was tested at the APS on the 1-ID beamline with a 10-keV monochromatic beam. The transmission at 10 keV is about 16%, which means that 16% of the flux on a 1-mm-diameter spot at the entrance to the lens emerged from the end of the lens. The focal spot remained slightly less than 40 microns for focal distances of 1400 to 1300 mm. The narrowest focus came at a distance of 1356 mm behind the lens, when the initial x-ray beam was collimated down to a square 0.4 mm  $\times$  0.4 mm and the lens was well aligned. This arrangement gave a focal spot of 33.6 microns. The lens

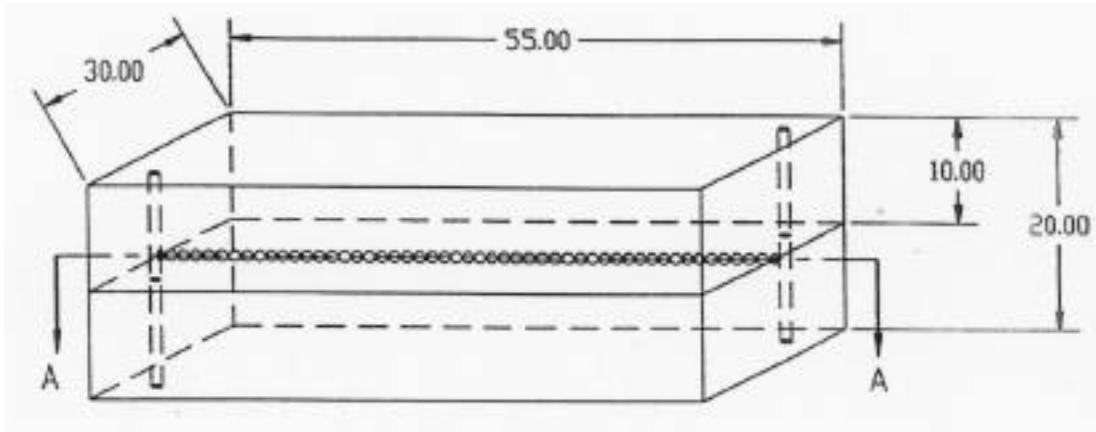


Fig. 5.27 Schematic of the Be refractive x-ray lens. It consists of 50 1-mm-diameter hollow spheres in a beryllium substrate. The web between each hollow sphere is 0.1 mm thick. All dimensions are in mm.

transmission for this smaller beam is approximately 30%. The theoretical value for the focal spot diameter was less than 10 microns. The wider spot diameter is believed to be due partly to the spherical shape of the hollow cavities, which causes focusing aberrations. This effect focuses the x-rays farther from the optical axis at shorter distances from the lens than the x-rays close to the optical axis of the lens, which was manifested through the best focus coming at a distance 100 cm shorter than the theoretical focal length of 1.466 m. Part of this shortening of the focal length could also be due to a slightly smaller diameter of the hollow spheres. The second factor that broadens the focal spot is the unevenness of the machining of the hollow sphere. This roughness was apparent when the half-hollow spheres were examined under a microscope. A method has been devised to eliminate the ridges in the surface of the hollow spheres and was tested on an aluminum lens (20 1-mm-diameter hollow spheres). The procedure consists of smoothing the hollow sphere surfaces using a special tool with a small amount of very fine polishing compound present while the

lens is submerged in water. This tool was also used to thin the wall between the hollow spheres of the Al lens, from 0.2 mm to 0.1 mm. This change improved the transmission of the aluminum lens by a factor of 5 at 30 keV.

### Gradient d-Spacing Crystals (Ge/Si and Si/Ge)

The width of the energy band diffracted by a perfect crystal is determined by the Darwin width of the crystal and/or by the divergence of the beam incident on the crystal. The energy spread due to the beam divergence can be eliminated by using a crystal whose d-spacing varies along the footprint of the incident beam such that the varying d-spacing compensates for the varying incident angles. Recently it has become possible to grow near-perfect crystals of Ge-Si mixtures, the d-spacing of which can be changed by varying the relative concentrations of the two components. Tests were performed on both single crystals of germanium with a small, varying

concentration of silicon and single crystals of silicon with a varying concentration of germanium grown by Nikolai Abrosimov at the Institute for Crystal Growth, Berlin. Both rocking curves and d-spacings were measured. The concentration of Si in the Ge/Si crystals varied from 0.1% to 2.6%, which changed the d-spacing by 0.104%. The rocking curves varied from 5 to 20 arc sec in the low Si region (less than 1% Si) and from 20 to 200 arc sec in the high Si region (greater than 1% Si). The concentration of Ge in the two Si/Ge crystals was 3.0% and 3.9%. The rocking curves (FWHM) varied from 40 arc sec to 50 arc sec in the 3.9% Ge crystal and from 60 to 120 arc sec in the 3.0% Si crystal. Thus the rocking curves appear to be more sensitive to the parameters and conditions used during the growing of these crystals than to the concentration of Si. A 4% change in the concentration of Ge will change the d-spacings by 0.16%. This would correspond to 67 arc sec at 10 keV for the [111] planes in silicon. At 30 m, this corresponds to a vertical height of 10 mm; thus a change in concentration of 1% or less will be sufficient for most synchrotron applications. Crystals with concentration changes of Ge of 1% or less have been grown with mosaic structure widths of a few arc sec and, thus, should be useful in synchrotron experiments.

### **Crystal Lenses for Medical Imaging**

A short focal length crystal diffraction lens has been developed for medical imaging applications. The lens is designed to focus the 141-keV gamma ray from  $^{99m}\text{Tc}$ , which is injected into the blood stream of cancer patients. Fast growing cancer cells will incorporate more of the radioactivity than normal cells. A full body scan is then made to locate possible cancer sites in the body.

The new medical lens will be used to verify the presence of these enhanced sites and obtain a 3-D image of the cancer. This 3D image will greatly simplify the taking of tissue samples and help guide subsequent surgery. The lens system will also be able to reject those borderline indications in the full body scan that are false and eliminate unnecessary tissue sampling. The lens is constructed of small copper crystals 4 mm by 4 mm on a side and 2 to 3 mm thick, mounted in rings such that each ring uses a different set of crystalline planes to diffract and focus the gamma rays. The focal length of this lens for the 141-keV  $^{99m}\text{Tc}$  line is 50 cm. The patient will be located 100 cm (two focal lengths) from the lens, and the detector will be located 100 cm behind the lens. Scanning on and off the cancer site will be done by moving the patient.

### **Crystal Lenses for Astrophysical Applications**

An international collaboration (U.S., France, England, Italy, and Germany) has been formed to perform a series of astrophysics balloon experiments that use a crystal diffraction lens to look at gamma rays from distant super nova remnants and other distant astrophysics sources. The lens will use Ge and Ge/Si crystals and will be constructed at the CERN laboratory in Toulouse, France. Argonne has supplied the Ti-Al alloy lens frame and support structure, as well as the design and technology needed to mount and align the lens crystals. Argonne will also be supporting this effort by making measurement of the diffraction efficiency of different mosaic crystals. Measurements have been made on crystals of Ge, Ge/Si, and Cu. The first samples of Mo and W crystals are expected in Nov. 1998.